Radboud Repository

Radboud University Nijmegen

PDF hosted at the Radboud Repository of the Radboud University Nijmegen

The following full text is a publisher's version.

For additional information about this publication click this link.
http://hdl.handle.net/2066/33312

Please be advised that this information was generated on 2020-11-01 and may be subject to change.

HTML ABSTRACT + LINKS

Ab initio computed diabatic potential energy surfaces of OH–HCl

Paul E. S. Wormer, Jacek A. Kłos,[a] Gerrit C. Groenenboom, and Ad van der Avoird[b]
Theoretical Chemistry, IMM, Radboud University Nijmegen, Toernooiveld 1, 6525 ED Nijmegen, The Netherlands

(Received 14 April 2005; accepted 17 May 2005; published online 6 July 2005)

The two four-dimensional diabatic potential energy surfaces (DPESs) for OH–HCl are computed that correlate with the twofold degenerate $^2\Pi$ ground state of the free OH radical. About 20 000 points on the surface are obtained by the *ab initio* coupled-cluster and multi-reference configuration interaction methods. Analytic forms for the diabatic potential energy surfaces are derived as expansions in complete sets of orthogonal functions depending on the three intermolecular angles. The numeric computation of the angular expansion coefficients is discussed. The distance-dependence of the angular coefficients is represented by the reproducing kernel Hilbert space method. It is checked that both diabatic potentials converge for large intermolecular separations to the values computed directly from the electrostatic multipole expansion. The final DPESs are discussed and illustrated by some physically meaningful one- and two-dimensional cuts through them. © *2005 American Institute of Physics*. [DOI: 10.1063/1.1949198]

I. INTRODUCTION

The abundant OH($^2\Pi$) radical is very reactive and known to take part in many atmospheric and combustion processes. Reactions of OH with the hydrogen halides efficiently convert halogens to their active forms. In particular, the reaction $OH+HCl \rightarrow H_2O+Cl$ is an important source of active chlorine in the atmosphere. Several experimental and computational studies have been devoted to this reaction, see Ref. 1 for a survey of the literature. An important aspect of the theoretical studies[2–6] is the potential energy surface for the reaction which was investigated either through the use of semi-empirical models or by means of *ab initio* electronic structure calculations. Most of these studies concentrate on the transition state for the reaction. In the article of Yu and Nyman[2] it is pointed out that a stable OH–HCl van der Waals complex occurs in the entrance channel of the reaction. Since it is known from theoretical work[7] on the analogous reaction $O+HCl \rightarrow OH+Cl$ that the existence of such a complex may have a large influence on the energy dependent reaction probabilities, detailed spectroscopic studies on the OH–HCl complex will be undertaken.[8] Also rotationally inelastic state-to-state scattering cross sections of OH($^2\Pi_{3/2}$) in collision with HCl were measured recently.[1] To support this experimental work, computations on the same cross sections are underway in our group. In addition, computations on the bound states of the van der Waals complex OH($^2\Pi$)–HCl are planned. The comparison of experimental and theoretical cross sections gives a thorough check on computed results and contributes importantly to the understanding of the physical origin of propensity rules observed in Ref. 1. The scattering and bound state calculations are based on the expanded potential energy surfaces reported in the present article.

A problem that occurs for many open-shell van der Waals molecules, including OH($^2\Pi$)–HCl, is the breakdown of the Born–Oppenheimer (BO) approximation. The BO approximation is applicable when the eigenvalues of the electronic Hamiltonian are everywhere (as function of the intermolecular nuclear coordinates) well separated in energy. However, for linear geometries of OH–HCl as well as for large intermolecular distances, the adiabatic states that correlate with the Π state of OH become degenerate, i.e., two potential energy surfaces (PESs) come close or even coincide. Terms arising from the nuclear kinetic energy operator, neglected in the BO approximation, are then no longer negligible. A solution for this problem was pointed out by Smith,[9] who introduced the concept of diabatic states. Diabatic states are linear combinations of adiabatic states—which by definition are eigenstates of the electronic Hamiltonian—that minimize (or annihilate) the non-BO nuclear kinetic coupling terms concurring with approaching PESs. The introduction of diabatic states is at the expense of giving a non-diagonal PES matrix and, correspondingly, it leads to multiple nuclear motion equations that are coupled by potential energy terms. Since we have here two orthonormal adiabatic states from which two orthonormal diabatic states are constructed, the transformation between them is completely specified by one rotation angle: "the diabatic angle" γ. As is explained in more detail below, we compute this angle by inspection of molecular orbitals and the lowest two multireference configuration interaction (MRCI) states.

It is known from much work on closed-shell van der Waals molecules that the coupled-cluster-singles-doubles plus non-iterative triples [CCSD(T)] approach is at present the most reliable supermolecule method for the computation of PESs. For open-shell complexes the partially spin-restricted CCSD(T) [RCCSD(T)] method is therefore an obvious choice. However, for most points on the PES a dimer

[a]Present address: Department of Chemistry & Biochemistry, University of Maryland, College Park, Maryland 20742-4454.
[b]Electronic mail: A.vanderAvoird@theochem.ru.nl

 © 2005 American Institute of Physics

Downloaded 01 Jun 2012 to 131.174.17.23. Redistribution subject to AIP license or copyright; see http://jcp.aip.org/about/rights_and_permissions

consisting of two diatoms has no point group symmetry and accordingly RCCSD(T) is strictly speaking only suitable to give the ground state energy. This is regrettable as the RCCSD(T) method is size-extensive, while most CI methods are not. As we just pointed out, the diabatic angle γ will be extracted from MRCI wave functions, so that MRCI calculations are required anyway. Therefore, to alleviate the size-extensivity problem, we computed ground state energies by the RCCSD(T) method and used the MRCI method for the first excitation energy ΔE_{MRCI}.

The outline of the paper is as follows: First we introduce the concept of diabatic potential energy surfaces (DPESs). Then we introduce an analytic expansion of these surfaces, which is suggested by long range theory and is appropriate for coupled-channel scattering and bound-state calculations. This is followed by a discussion of the practical details of the calculations. Finally we give the results and present some illustrative cuts through the diabatic and adiabatic potentials.

II. THEORY

A. Diabatic potentials

Under influence of the interaction the rotational symmetry of OH is broken and the degeneracy of the Π states is lifted, because they are contaminated by states of symmetry other than Π. This is a second-order effect. In first-order in the interaction, Π_x and Π_y are mixed in a definite manner. To a good approximation we can therefore write the two broken-symmetry adiabatic states Ψ_1 and Ψ_2, with interaction energies V_1 and V_2, as a linear combination of pure Π_x and Π_y states,

$$(|\Pi_x\rangle,|\Pi_y\rangle) = (|\Psi_1\rangle,|\Psi_2\rangle)\mathbb{R}(\gamma)$$
$$\text{with } \mathbb{R}(\gamma) \equiv \begin{pmatrix} \cos\gamma & -\sin\gamma \\ \sin\gamma & \cos\gamma \end{pmatrix}. \tag{1}$$

Since the diabatic states Π_x and Π_y are monomer states, they give vanishing distance-dependent (radial) nuclear kinetic coupling terms. If the expression (1) for the adiabatic states were exact, the coupling terms would be transformed away by this equation. In any case, we assume the radial coupling terms to become so small by this transformation that they can be neglected in the nuclear motion problem. Transformation of the (diagonal) adiabatic energy matrix gives

$$\mathbb{R}(\gamma)^T \begin{pmatrix} V_1 & 0 \\ 0 & V_2 \end{pmatrix} \mathbb{R}(\gamma) = \frac{V_1+V_2}{2}\begin{pmatrix} 1 & 0 \\ 0 & 1 \end{pmatrix} + \frac{V_2-V_1}{2}\begin{pmatrix} -\cos 2\gamma & \sin 2\gamma \\ \sin 2\gamma & \cos 2\gamma \end{pmatrix}. \tag{2}$$

The diabatic angle γ, which is a function of the intermolecular coordinates, can be determined from the *ab initio* states Ψ_1 and Ψ_2 via Eq. (1). Use of the eigenstates $|\Lambda\rangle$ with $\Lambda = \pm 1$ of $\hat{L}_z$, the projection of the electronic angular momentum on the O–H axis, gives the required reduction of the azimuthal nuclear kinetic coupling terms.[10] The states $|\Lambda\rangle$ are simply related to the diabatic states $|\Pi_x\rangle$ and $|\Pi_y\rangle$

$$(|1\rangle,|-1\rangle) \equiv \frac{1}{\sqrt{2}}(|\Pi_x\rangle,|\Pi_y\rangle)\begin{pmatrix} -1 & 1 \\ -i & -i \end{pmatrix} \tag{3}$$

and further transformation of the energy matrix gives

$$\begin{pmatrix} V_{-1,-1} & V_{-1,1} \\ V_{1,-1} & V_{1,1} \end{pmatrix} = \frac{1}{2}\begin{pmatrix} V_1+V_2 & (V_2-V_1)\exp(-2i\gamma) \\ (V_2-V_1)\exp(2i\gamma) & V_1+V_2 \end{pmatrix}. \tag{4}$$

We will refer to the matrix elements $V_{\pm 1,\pm 1}$ as *diabatic potential energy surfaces* (DPESs).

For planar geometries the adiabatic states $|\Psi_1\rangle$ and $|\Psi_2\rangle$ have A'/A'' (even/odd) symmetry with respect to reflection in the plane of the complex. Except when the OH radical lies along the intermolecular bond axis, they must coincide with the diabatic states $|\Pi_x\rangle$ and $|\Pi_y\rangle$ and the diabatic angle γ equals 0° or 90°. When the OH radical lies along the bond axis the angle γ is determined by the orientation of the plane through the HCl axis and the bond axis. This will be discussed in more detail below.

The use of the diabatic states $|\Lambda\rangle = |\pm 1\rangle$ is very convenient also for the inclusion of spin-orbit coupling in bound state and scattering calculations on the OH–HCl complex. Spin-orbit coupling in the $X\,^2\Pi$ ground state of the OH radical can be represented by the operator $A\hat{L}_z\hat{S}_z$ with a coupling constant $A = -139.21\ \mathrm{cm}^{-1}$. The operator $\hat{L}_z$ is diagonal in the basis $|\Lambda\rangle$ with eigenvalues $\Lambda = \pm 1$ and $\hat{S}_z$ is diagonal in the spin basis $|\pm\frac{1}{2}\rangle$, so that only a diagonal term $\pm A/2$ has to be added to the diabatic potential matrix in Eq. (4) for the spin-orbit coupled eigenstates $|^2\Pi_{3/2}\rangle$ and $|^2\Pi_{1/2}\rangle$ of $\hat{j}_z = \hat{L}_z + \hat{S}_z$.

B. Expansion of DPESs for two interacting open-shell diatoms

We now present an expansion of DPESs for two open-shell diatoms. Although in this paper we are studying the case of one open- and one closed-shell diatomic molecule, the generalization to two open-shell diatoms is easy and natural. This expansion will be derived from the first-order (in the interaction V) long-range (no exchange) perturbation matrix. In the long range diabatic states are equal to products of monomer (zeroth-order) states. The general expansion, derived in this section for the matrix elements of the first-order perturbation matrix, is in principle exact, as it is an expansion in a complete basis. There are, however, an infinite number of complete expansion bases. The expansion basis chosen here has the important advantage that the matrix elements go continuously over into the correct large R expressions and the correct expressions for linear dimer geometries.

Let us first consider one rigid diatom with its molecular axis parallel to the z-axis of an arbitrarily oriented space-fixed (SF) frame. Its electronic wave functions $|\Lambda\rangle$ are adapted to $C_{\infty v}$,

$$\hat{R}_z(\psi)|\Lambda\rangle \equiv e^{-i\psi\hat{L}_z}|\Lambda\rangle = e^{-i\psi\Lambda}|\Lambda\rangle. \tag{5}$$

Reflection $\hat{\sigma}_{xz}$ in the xz-plane is represented in the basis $|\pm|\Lambda|\rangle$ by

Downloaded 01 Jun 2012 to 131.174.17.23. Redistribution subject to AIP license or copyright; see http://jcp.aip.org/about/rights_and_permissions

$$(-1)^{\Lambda}\begin{pmatrix}0 & 1\\ 1 & 0\end{pmatrix}, \tag{6}$$

where the phase is a matter of convention. Rotate now the vector $\mathbf{r}$, pointing from one nucleus of the diatom to the other, to its desired orientation given by polar coordinates θ and ϕ with respect to the SF frame. This requires the active rotation $\hat{R}(\theta,\phi)\equiv\hat{R}_{y'}(\theta)\hat{R}_z(\phi)$ of $\mathbf{r}$, which initially was parallel to the SF z-axis. In order to keep electrons and nuclei in the same relative position we must rotate the electronic wave function in the very same way,

$$\hat{R}_{y'}(\theta)\hat{R}_z(\phi)|\Lambda\rangle \equiv |\Lambda(\theta,\phi)\rangle. \tag{7}$$

Note that rotation over ψ around the rotated diatomic axis z'' still gives the factor $\exp(-i\psi\Lambda)$,

$$\begin{aligned} &e^{-i\psi\hat{L}_{z''}}|\Lambda(\theta,\phi)\rangle = e^{-i\psi\Lambda}|\Lambda(\theta,\phi)\rangle\\ &\text{where } \hat{L}_{z''}\equiv\hat{R}(\theta,\phi)\hat{L}_z\hat{R}(\theta,\phi)^{\dagger}, \end{aligned} \tag{8}$$

because

$$\hat{L}_{z''}|\Lambda(\theta,\phi)\rangle = \hat{R}(\theta,\phi)\hat{L}_z|\Lambda(0,0)\rangle = \Lambda|\Lambda(\theta,\phi)\rangle, \tag{9}$$

with $|\Lambda(0,0)\rangle\equiv|\Lambda\rangle$. Hence, the most general electronic wave function obtained by a three-angle Euler rotation $\hat{R}(\psi,\theta,\phi)\equiv\hat{R}_{z''}(\psi)\hat{R}_{y'}(\theta)\hat{R}_z(\phi)$ is

$$|\Lambda(\psi,\theta,\phi)\rangle = \hat{R}(\psi,\theta,\phi)|\Lambda\rangle = e^{-i\psi\Lambda}|\Lambda(\theta,\phi)\rangle. \tag{10}$$

We will keep using also the two-angle notation of the electronic wave functions, which should be understood as $|\Lambda(\theta,\phi)\rangle\equiv|\Lambda(0,\theta,\phi)\rangle$.

Let us next consider two diatoms A and B with Euler angles (ψ_A,θ_A,ϕ_A) and (ψ_B,θ_B,ϕ_B) with respect to the same SF frame. In first-order perturbation theory one constructs a matrix of the interaction operator $V\equiv H-H_A-H_B$ with zeroth-order bra and ket that are products of the degenerate monomer states. Rotating each of the diatoms and assuming that the vector $\mathbf{R}$ pointing from A to B has the SF polar angles (Θ,Φ), we find that the matrix element

$$\begin{aligned} \tilde{V}_{\Lambda_A'\Lambda_B'\Lambda_A\Lambda_B} &\equiv \langle\Lambda_A'(\psi_A,\theta_A,\phi_A)\Lambda_B'(\psi_B,\theta_B,\phi_B)|\\ &\quad\times V|\Lambda_A(\psi_A,\theta_A,\phi_A)\Lambda_B(\psi_B,\theta_B,\phi_B)\rangle\\ &= e^{i\psi_A(\Lambda_A'-\Lambda_A)+i\psi_B(\Lambda_B'-\Lambda_B)}\langle\Lambda_A'(\theta_A,\phi_A)\Lambda_B'(\theta_B,\phi_B)|\\ &\quad\times V|\Lambda_A(\theta_A,\phi_A)\Lambda_B(\theta_B,\phi_B)\rangle\\ &\equiv e^{i\psi_A(\Lambda_A'-\Lambda_A)i\psi_B(\Lambda_B'-\Lambda_B)}V_{\Lambda_A'\Lambda_B'\Lambda_A\Lambda_B} \end{aligned} \tag{11}$$

is a function of two sets of Euler angles, one for diatom A and one for diatom B, and of the polar angles Φ and Θ. By the Peter–Weyl theorem[11] the matrix element can be expanded in products of rigid rotor functions (complex conjungates of Wigner D-matrices) and spherical harmonic functions $C_M^L(\Theta,\Phi)^*$,

$$\begin{aligned} \tilde{V}_{\Lambda_A'\Lambda_B'\Lambda_A\Lambda_B} &= \sum_{L_AM_AK_A}\sum_{L_BM_BK_B}\sum_{LM} C^{\Lambda_A'\Lambda_B'\Lambda_A\Lambda_B}_{L_AM_AK_AL_BM_BK_BLM}(R)\\ &\quad\times D^{L_A}_{M_AK_A}(\phi_A,\theta_A,\psi_A)^*\\ &\quad\times D^{L_B}_{M_BK_B}(\phi_B,\theta_B,\psi_B)^* C_M^L(\Theta,\Phi)^*. \end{aligned} \tag{12}$$

Equating factors containing ψ_A and ψ_B, while realizing that the complex conjugate D-matrices contain $\exp(iK_A\psi_A)$ and $\exp(iK_B\psi_B)$, shows that $K_A=\Lambda_A'-\Lambda_A$ and $K_B=\Lambda_B'-\Lambda_B$, so that the summations over K_A and K_B each shrink to one term.

Any matrix element of an energy operator is invariant under any rotation $\hat{R}$ of all its integration variables (the electron coordinates), because a rotation is unitary, so that $\langle\Phi|V|\Psi\rangle=\langle\Phi|\hat{R}^{\dagger}\hat{R}V\hat{R}^{\dagger}\hat{R}|\Psi\rangle=\langle\hat{R}\Phi|V|\hat{R}\Psi\rangle$. The fact that the matrix element is a rotational invariant implies that it is useful to Clebsch–Gordan couple the right-hand-side of Eq. (12). The elements $(D^j_{mk})^*$ of column k transform as spherical harmonic functions C^j_m and accordingly it can be shown by an argument, similar to the one used in the proof of the Wigner–Eckart theorem, that the expansion in terms of invariants becomes

$$\begin{aligned} V_{\Lambda_A'\Lambda_B'\Lambda_A\Lambda_B} &= \sum_{L_A}\sum_{L_B}\sum_{L} v^{\Lambda_A'\Lambda_B'\Lambda_A\Lambda_B}_{L_AL_BL}(R)\\ &\quad\times\sum_{M_AM_BM}\langle L,M|L_A,M_A;L_B,M_B\rangle\\ &\quad\times D^{L_A}_{M_A,\Lambda_A'-\Lambda_A}(\phi_A,\theta_A,0)^*\\ &\quad\times D^{L_B}_{M_B,\Lambda_B'-\Lambda_B}(\phi_B,\theta_B,0)^* C_M^L(\Theta,\Phi)^*. \end{aligned} \tag{13}$$

Note that the angles ψ_A and ψ_B involved only in the rotation of the electron coordinates of the diatoms around the molecular axes have dropped out from this expression. The potential matrix elements $V_{\Lambda_A'\Lambda_B'\Lambda_A\Lambda_B}$ defined in Eq. (11) are integrals over electronic wave functions $|\Lambda_A(\theta_A,\phi_A)\rangle$ and $|\Lambda_B(\theta_B,\phi_B)\rangle$ and the electron coordinates are integration variables.

C. Properties of expansion coefficients

From certain invariances follow a few important properties of the expansion coefficients $v^{\Lambda_A'\Lambda_B'\Lambda_A\Lambda_B}_{L_AL_BL}$ appearing in Eq. (13). In the first place the operator V is invariant under inversion of all particles (electrons and nuclei) with respect to an arbitrary point in space. If we choose the origin of the SF frame as inversion point, this operation can be expressed as a reflection $\hat{\sigma}_{xz}$ in the xz-plane of the SF frame times an overall rotation around the SF y-axis. Since we already saw that V is invariant under any overall rotation, we consider only the effect of $\hat{\sigma}_{xz}$. For the azimuthal angle of the three nuclear vectors $\mathbf{r}_A,\mathbf{r}_B$, and $\mathbf{R}$ this reflection gives the map $\phi\mapsto-\phi$, hence for diatom X (X=A,B) holds

$$\hat{\sigma}_{xz}|\Lambda(\theta_X,\phi_X)\rangle = \hat{R}(\theta_X,-\phi_X)\hat{\sigma}_{xz}|\Lambda(0,0)\rangle, \tag{14}$$

so that Eq. (6) gives

Downloaded 01 Jun 2012 to 131.174.17.23. Redistribution subject to AIP license or copyright; see http://jcp.aip.org/about/rights_and_permissions

$$\hat{\sigma}_{xz}|\Lambda_A(\theta_A,\phi_A)\Lambda_B(\theta_B,\phi_B)\rangle = (-1)^{\Lambda_A+\Lambda_B}|-\Lambda_A(\theta_A,-\phi_A),-\Lambda_B(\theta_B,-\phi_B)\rangle. \quad (15)$$

Hence,

$$V_{\Lambda'_A\Lambda'_B\Lambda_A\Lambda_B} = (-1)^{\Lambda'_A\Lambda'_B\Lambda_A\Lambda_B} \times\langle-\Lambda'_A(\theta_A,-\phi_A),-\Lambda'_B(\theta_B,-\phi_B)| \times V|-\Lambda_A(\theta_A,-\phi_A),-\Lambda_B(\theta_B,-\phi_B)\rangle. \quad (16)$$

Expand the right-hand side according to Eq. (13) and substitute in this expansion

$$D^l_{m,k}(-\phi,\theta,0)^* = (-1)^{k+m}D^l_{-m,-k}(\phi,\theta,0)^*, \quad (17)$$

$$C^L_M(\Theta,-\Phi)^* = (-1)^M C^L_{-M}(\Theta,\Phi)^*, \quad (18)$$

and (for integer L,M)

$$\langle L,-M|L_A,-M_A;L_B,-M_B\rangle(-1)^{M_A+M_B+M} = (-1)^{L_A+L_B+L}\langle L,M|L_A,M_A;L_B,M_B\rangle \quad (19)$$

followed by equating the terms in this expansion with those in the expansion of the noninverted matrix element. In this manner we get the symmetry property

$$v^{\Lambda'_A\Lambda'_B\Lambda_A\Lambda_B}_{L_AL_BL} = (-1)^{L_A+L_B+L}v^{-\Lambda'_A,-\Lambda'_B,-\Lambda_A,-\Lambda_B}_{L_AL_BL}. \quad (20)$$

In a very similar manner follows from $V^\dagger = V$ that

$$v^{\Lambda'_A\Lambda'_B\Lambda_A\Lambda_B}_{L_AL_BL} = (-1)^{L_A+L_B+L}\left(v^{\Lambda_A\Lambda_B\Lambda'_A\Lambda'_B}_{L_AL_BL}\right)^*, \quad (21)$$

where we used that the Λ dependent phase is one since $|\Lambda'_X| = |\Lambda_X|$. And from invariance under time reversal[12]

$$v^{\Lambda'_A\Lambda'_B\Lambda_A\Lambda_B}_{L_AL_BL} = (-1)^{L_A+L_B+L}\left(v^{-\Lambda'_A,-\Lambda'_B,-\Lambda_A,-\Lambda_B}_{L_AL_BL}\right)^*. \quad (22)$$

Combining the last three equations gives

$$v^{\Lambda'_A\Lambda'_B\Lambda_A\Lambda_B}_{L_AL_BL} = \left(v^{-\Lambda_A,-\Lambda_B,-\Lambda'_A,-\Lambda'_B}_{L_AL_BL}\right)^* = \left(v^{\Lambda'_A\Lambda'_B\Lambda_A\Lambda'_B}_{L_AL_BL}\right)^*. \quad (23)$$

In particular, we see that all expansion coefficients are real.

The expansion coefficients of the diagonal potentials with $\Lambda'_A = \Lambda_A$ and $\Lambda'_B = \Lambda_B$ obey the relation

$$v^{\Lambda_A\Lambda_B\Lambda_A\Lambda_B}_{L_AL_BL}(R) = (-1)^{L_A+L_B+L}v^{\Lambda_A\Lambda_B\Lambda_A\Lambda_B}_{L_AL_BL}(R) \quad (24)$$

and, hence, they must vanish for odd values of L_A+L_B+L.

D. Open-plus closed-shell diatom

We specialize the earlier results to the case that A is open-shell and B is closed-shell with the centers of mass of both diatoms lying on the z-axis of the SF frame. If we first rotate the total dimer such that **R** is along the z-axis of the SF system, $\Theta=\Phi=0$, we have for the Racah normalized spherical harmonic

$$C^L_M(\Theta,\Phi) = \delta_{M0}, \quad (25)$$

so that the expansion (13) for two open-shell diatoms becomes

$$V_{\Lambda'_A\Lambda'_B\Lambda_A\Lambda_B}(R,\theta_A,\theta_B,\phi_A-\phi_B) = \sum_{L_AL_BL} v^{\Lambda'_A\Lambda'_B\Lambda_A\Lambda_B}_{L_AL_BL}(R)\sum_M \langle L,0|L_A,M;L_B,-M\rangle \times D^{L_A}_{M,\Lambda'_A-\Lambda_A}(\phi_A,\theta_A,0)^* D^{L_B}_{-M,\Lambda'_B-\Lambda_B}(\phi_B,\theta_B,0)^*. \quad (26)$$

Take now diatom B (HCl) in a Σ state: $\Lambda'_B=\Lambda_B=0$. Use

$$D^{L_B}_{-M,0}(\phi_B,\theta_B,0)^* = C^{L_B}_{-M}(\theta_B,\phi_B)$$

and we get, suppressing Λ_B and Λ'_B in the notation and dropping the subscript A on the Λs,

$$V_{\Lambda'\Lambda} = \sum_{L_AL_BL} v^{\Lambda'\Lambda}_{L_AL_BL}(R)\sum_M \langle L,0|L_A,M;L_B,-M\rangle \times D^{L_A}_{M,\Lambda'-\Lambda}(\phi_A,\theta_A,0)^* C^{L_B}_{-M}(\theta_B,\phi_B). \quad (27)$$

We see that the diagonal elements $V_{1,1}=V_{-1,-1}$ of Eq. (4), which are real, are expanded in terms of $D^{L_A}_{M,0}(\phi_A,\theta_A,0)^* = C^{L_A}_M(\theta_A,\phi_A)$ (times spherical harmonics for B), while the expansion of the complex-valued off-diagonal elements $V_{1,-1}$ contains the functions $D^{L_A}_{M,2}(\phi_A,\theta_A,0)^*$.

E. Alternative expansion

In some cases, for example, if the potential is available on a grid of points (θ_A,θ_B,ϕ) and the number of ϕ points is smaller than the number of θ_A and θ_B points, it is convenient to expand the potential in uncoupled functions. We restrict our attention to the case of an open-shell diatom (A) in interaction with a closed-shell diatom (B) and rewrite Eq. (27),

$$V_{\Lambda'\Lambda} = \sum_{L_AL_BM} v^{\Lambda'\Lambda}_{L_AL_BM}(R)D^{L_A}_{M,\Lambda'-\Lambda}(\phi_A,\theta_A,0)^* C^{L_B}_{-M}(\theta_B,\phi_B), \quad (28)$$

with

$$v^{\Lambda'\Lambda}_{L_AL_BM}(R) \equiv \sum_L v^{\Lambda'\Lambda}_{L_AL_BL}(R)\langle L,0|L_A,M;L_B,-M\rangle. \quad (29)$$

Given the coefficients $v^{\Lambda'\Lambda}_{L_AL_BM}(R)$ that we refer to as "*LLM* coefficients", the "*LLL* coefficients" $v^{\Lambda'\Lambda}_{L_AL_BL}(R)$ follow from the unitarity of the Clebsch–Gordan coefficients,

$$v^{\Lambda'\Lambda}_{L_AL_BL} = \sum_M \langle L,0|L_A,M;L_B,-M\rangle v^{\Lambda'\Lambda}_{L_AL_BM}. \quad (30)$$

From Eqs. (20)–(22) it follows that the *LLM* expansion coefficients must obey

$$v^{\Lambda',\Lambda}_{L_A,L_B,M}(R) = v^{-\Lambda',-\Lambda}_{L_A,L_B,-M}(R) \quad (31)$$

$$v^{\Lambda',\Lambda}_{L_A,L_B,M}(R) = v^{\Lambda,\Lambda'}_{L_A,L_B,-M}(R)^* \quad (32)$$

$$v^{\Lambda',\Lambda}_{L_A,L_B,M}(R) = v^{-\Lambda',-\Lambda}_{L_A,L_B,-M}(R)^*. \quad (33)$$

Combining these equations one finds again that all expansion coefficients must be real-valued

Downloaded 01 Jun 2012 to 131.174.17.23. Redistribution subject to AIP license or copyright; see http://jcp.aip.org/about/rights_and_permissions

$$v^{\Lambda',\Lambda}_{L_A L_B M}(R) = v^{\Lambda',\Lambda}_{L_A L_B M}(R)^*, \tag{34}$$

which is also obvious from Eq. (30). Furthermore, the diagonal potentials $V_{-\Lambda,-\Lambda}(R,\theta_A,\theta_B,\phi)$ and $V_{\Lambda,\Lambda}(R,\theta_A,\theta_B,\phi)$ have equal expansion coefficients

$$v^{-\Lambda,-\Lambda}_{L_A L_B M}(R) = v^{\Lambda,\Lambda}_{L_A L_B M}(R). \tag{35}$$

The expansion coefficients with $\Lambda'=\Lambda$ for $-M$ and $+M$ are equal as well

$$v^{\Lambda,\Lambda}_{L_A,L_B,M}(R) = v^{\Lambda,\Lambda}_{L_A,L_B,-M}(R) \tag{36}$$

and by combining the terms with $-M$ and $+M$ in the expansion of Eq. (28) we obtain an expansion of the diagonal potentials in terms of real-valued angular functions

$$V_{\Lambda,\Lambda}(R,\theta_A,\theta_B,\phi) = \sum_{L_A L_B} \sum_{M\geqslant 0} (2-\delta_{M0})(-1)^M \times v^{\Lambda,\Lambda}_{L_A L_B M}(R) C^{L_A}_M(\theta_A,0) C^{L_B}_M(\theta_B,0)\cos M\phi. \tag{37}$$

Here, we used $D^L_{M0}(0,\theta,0) \equiv d^L_{M,0}(\theta) = C^L_M(\theta,0)$ and $C^L_{-M}(\theta,0) = (-1)^M C^L_M(\theta,0)$.

F. Multipole expansion

For large distances R between two molecules we can write the intermolecular interaction operator V in the form of the multipole expansion

$$V = \sum_{L_A,L_B=0}^{\infty} (-1)^{L_B} \begin{pmatrix} 2L_A+2L_B \\ 2L_A \end{pmatrix}^{1/2} R^{-L_A-L_B-1} \times \sum_{M_A=-L_A}^{L_A} \sum_{M_B=-L_B}^{L_B} (-1)^{M_A+M_B} \times \langle L_A,M_A;L_B,M_B | L_A+L_B, M_A+M_B\rangle \times Q^{L_A}_{M_A} Q^{L_B}_{M_B} C^{L_A+L_B}_{-(M_A+M_B)}(\Theta,\Phi), \tag{38}$$

where $Q^{L_A}_{M_A}$ and $Q^{L_B}_{M_B}$ are spherical multipole operators depending on the electronic and nuclear coordinates of the diatoms A and B, respectively. The vector $\mathbf{R}=(R,\Theta,\Phi)$ points from A to B. Since multipole operators are irreducible tensor operators it follows for both diatoms that

$$Q^L_M(\theta,\phi) \equiv \hat{R}(\theta,\phi)^\dagger Q^L_M \hat{R}(\theta,\phi) = \sum_K Q^L_K D^L_{M,K}(\phi,\theta,0)^*. \tag{39}$$

For HCl in its Σ ground state only the $K_B=0$ component $\langle Q^{L_B}_0\rangle$ is nonvanishing, so that

$$\langle Q^{L_B}_{M_B}(\theta_B,\phi_B)\rangle = \langle Q^{L_B}_0\rangle D^{L_B}_{M_B 0}(\phi_B,\theta_B,0)^* = \langle Q^{L_B}_0\rangle C^{L_B}_{M_B}(\theta_B,\phi_B). \tag{40}$$

For OH (=A) we must evaluate matrix elements

$$\langle \Lambda'(\theta_A,\phi_A)|Q^{L_A}_{M_A}|\Lambda(\theta_A,\phi_A)\rangle = \langle \Lambda'(0,0)|\hat{R}(\theta_A,\phi_A)^\dagger Q^{L_A}_{M_A}\hat{R}(\theta_A,\phi_A)|\Lambda(0,0)\rangle = \langle \Lambda'(0,0)|Q^{L_A}_{\Lambda'-\Lambda}|\Lambda(0,0)\rangle D^{L_A}_{M_A,\Lambda'-\Lambda}(\phi_A,\theta_A,0)^*.$$

Computing matrix elements of Eq. (38) and taking $\mathbf{R}$ along the z-axis, so that $M_A=M=-M_B$, we find precisely the expansion of Eq. (27) with expansion coefficients expressed in closed form

$$v^{\Lambda'\Lambda}_{L_A L_B L}(R) = \delta_{L_A+L_B,L}(-1)^{L_B} \begin{pmatrix} 2L_A+2L_B \\ 2L_A \end{pmatrix}^{1/2} \langle \Lambda'|Q^{L_A}_{\Lambda'-\Lambda}|\Lambda\rangle \times \langle Q^{L_B}_0\rangle R^{-L_A-L_B-1}. \tag{41}$$

Hence, in first-order long range theory one can directly compute the DPESs $V_{\Lambda',\Lambda}(R,\theta_A,\theta_B,\phi)$. The long range diabatic angle γ can be extracted from the off-diagonal matrix element $V_{1,-1}$. This element is complex-valued and its phase angle equals 2γ, see Eq. (4).

Note that the dominant long-range contribution to the diagonal potentials $V_{1,1}=V_{-1,-1}$ in the OH-HCl complex is the dipole-dipole interaction which depends on the distance as R^{-3}. This term does not occur in the off-diagonal potentials $V_{1,-1}=V^*_{-1,1}$; the dominant long-range contribution to $V_{1,-1}$ is the quadrupole-dipole interaction proportional to R^{-4}, which contains the off-diagonal quadrupole matrix element $\langle \Pi_1|\hat{Q}^2_2|\Pi_{-1}\rangle$ of the OH radical in its $^2\Pi$ ground state. Also the higher multipole operators of OH provide such off-diagonal matrix elements.

III. COMPUTATIONS

As pointed out in the introduction, we computed the lowest energy by the RCCSD(T) method and the first excitation energy by the MRCI method. Accordingly, the adiabatic energies are defined thus,

$$V_1 \equiv E_{\mathrm{RCCSD(T)}}(\mathrm{OH-HCl}) - E_{\mathrm{RCCSD(T)}}(\mathrm{OH}) - E_{\mathrm{RCCSD(T)}}(\mathrm{HCl}),$$
$$V_2 \equiv V_1 + \Delta E_{\mathrm{MRCI}}, \tag{42}$$

the idea being that the unlinked cluster contributions in the lowest and second lowest MRCI state mutually cancel to a large extent. (Recall that the size-extensivity problem is caused by a contamination of the CI wave functions by unlinked clusters.) Davidson-corrected[13] energies were used throughout this work. To correct for basis set superposition errors the RCCSD(T) calculations were all performed in the dimer orbital basis, while we assume that the BSSEs in ΔE_{MRCI} mutually cancel.

In the RCCSD(T) calculations we used the augmented correlation-consistent polarized-valence double zeta (aug-cc-pVDZ)[14] basis enlarged with bond functions placed halfway between the centers of mass of OH and HCl. Exponents of these uncontracted functions are $sp(0.9,0.3,0.1)$ and $d(0.6,0.2)$. In the MRCI calculations the bond functions caused problems in extracting diabatic angles, which is why we discarded them and used the larger aug-cc-pVTZ basis

Downloaded 01 Jun 2012 to 131.174.17.23. Redistribution subject to AIP license or copyright; see http://jcp.aip.org/about/rights_and_permissions

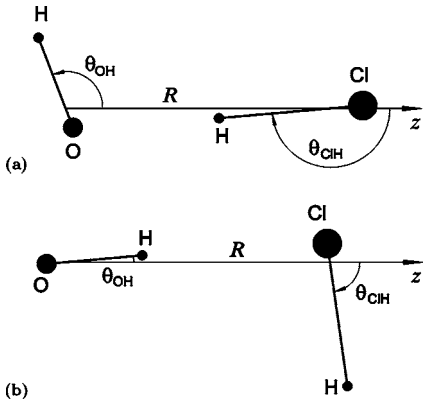

FIG. 1. Structure of global (a) and local (b) minimum in lowest adiabatic potential energy surface. Structure (a) has $\theta_{OH}=110.7°$, $\theta_{ClH}=176.4°$, $\phi=180°$, $R_e=3.366$ Å, and $D_e=1123$ cm^{-1}. Structure (b) has $\theta_{OH}=5.5°$, $\theta_{ClH}=86.9°$, $\phi=180°$, $R_e=3.517$ Å, and $D_e=655$ cm^{-1}.

instead. The 27-electron MRCI calculations were based on natural orbitals obtained from complete active space self-consistent field (CASSCF) calculations with 6 orbitals doubly occupied and 10 orbitals in the active space. Since the contracted MRCI calculations were used only to compute excitation energies and diabatic angles, they were kept fairly modest with 12 doubly occupied orbitals, 4 orbitals in the active space and 126 external orbitals. All calculations reported on in this work were performed by the aid of the program MOLPRO.[15]

The center of mass A of OH was placed in the origin, and the atomic masses are ^{1}H:1.0078250321 u, ^{16}O:15.9949146221 u. The O–H bond length of 1.950 a_0 was taken from earlier work[16,17] on the Ar–OH complex. The usual spherical polar angles of the vector r_{OH}, pointing from O to H, are denoted by θ_A and ϕ_A. The center of mass B of HCl was placed on the positive z-axis at R, the mass of ^{35}Cl (75.8% natural abundance) is 34.96885271 u. The H–Cl bond length of 1.275 Å (=2.4094 a_0) corresponds to the equilibrium distance.[18] The usual spherical polar angles of $\mathbf{r}_{ClH}$, pointing from Cl to H, are denoted by θ_B and ϕ_B. Figure 1, which shows the equilibrium geometries of the OH–HCl dimer (discussed below), illustrates the coordinates. The computations were performed for 24 distances: $R=25$, 22, 20, 18, 14, 10, 8, 6, 5, 4.5, 4.25, 4, 3.75, 3.5, 3.25, 3.15, 3.05, 3, 2.75, 2.65, 2.5, 2.35, 2.25, and 2 Å. The angles θ_A and θ_B were varied over 0°, 15°, 30°, 45°, 60°, 80°, 90°, 100°, 120°, 135°, 150°, 165°, and 180°, while the dihedral angle $\phi \equiv \phi_B - \phi_A$ was varied from 0° to 180° in steps of 45°. In total we computed 20280 points on the PES. (Actually, in this number a few geometries are counted more than once. For instance, when HCl is along the z-axis the interaction does not depend on ϕ.)

In order to extract the diabatic angle γ from natural orbitals and CI vectors by Eq. (1), it is necessary to first let the diatomic OH axis coincide with the SF z-axis. We used $\phi_A=0$ (OH in xz-plane) and $\phi=\phi_B$ so that it is required to rotate the vectors $\mathbf{R}, \mathbf{r}_{ClH}$, and $\mathbf{r}_{OH}$ actively around the y-axis over an angle $-\theta_A$. This rotation was performed on the Cartesian input vectors to the MOLPRO program. Next we must realize that the two lowest CI vectors, Ψ_1 and Ψ_2, are linear combinations of two dominant configuration state functions (CSFs), which can be seen as states with a hole in a π_1 and π_2 natural orbital created out of a closed-shell reference state $|\Phi_0\rangle$. Of course, CSFs of non-Π symmetry contribute to Ψ_1 and Ψ_2 as well, but as already discussed, these are of minor importance. The two highest occupied natural orbitals are given to a very good approximation by

$$(|\pi_1\rangle, |\pi_2\rangle) = (|\pi_x\rangle, |\pi_y\rangle)\mathbb{R}(\gamma_{orb}), \tag{43}$$

where π_x and π_y are linear combinations of p_x and p_y AOs, respectively. Introducing corresponding hole creation operators $a_1^\dagger$ and $a_2^\dagger$, we can write the CI vectors (adiabatic states) in terms of the hole states $a_1^\dagger|\Phi_0\rangle$ and $a_2^\dagger|\Phi_0\rangle$,

$$\big(|\Psi_1\rangle, |\Psi_2\rangle\big) = (a_1^\dagger, a_2^\dagger)\mathbb{R}(\gamma_{CI})|\Phi_0\rangle. \tag{44}$$

According to Eq. (43) and realizing that for an orthogonal transformation particles and holes transform the same,

$$(a_1^\dagger, a_2^\dagger) = (a_x^\dagger, a_y^\dagger)\mathbb{R}(\gamma_{orb}) \tag{45}$$

so that

$$\big(|\Psi_1\rangle, |\Psi_2\rangle\big) = (a_x^\dagger, a_y^\dagger)\mathbb{R}(\gamma_{orb})\mathbb{R}(\gamma_{CI})|\Phi_0\rangle, \tag{46}$$

and $\gamma=\gamma_{orb}+\gamma_{CI}$.

By inspection of the dominant coefficients of the two highest natural orbitals and of the lowest two CI vectors the diabatic angles γ_{orb} and γ_{CI} can be obtained from Eqs. (43) and (44). In practice we put all non-relevant (small) coefficients in the two orbitals and in the two states equal to zero and re-orthonormalized the two orbitals and the two states, before extracting the diabatic angles. This re-orthonormalization was done by the Löwdin algorithm.[19] It was checked that the angles obtained by an alternative orthonormalization algorithm, the Gram–Schmidt method, did not differ from our values by more than four degrees, even for the shortest distances where Π symmetry breaking is largest. Substitution of γ and the adiabatic energies V_1 and V_2 [cf. Eq. (42)] into Eq. (4) gives finally the DPESs $V_{1,1}=V_{-1,-1}$ and $V_{1,-1}=V_{-1,1}^*$.

We also computed the diabatic potentials $V_{1,1}$ and $V_{1,-1}$ directly from the multipole expansion, see Eq. (41) for the expansion coefficients. The multipole matrix elements of OH in its $^2\Pi$ ground state and the multipole moments of HCl were calculated from MRCI wave functions with the MOLPRO program. The monomer basis sets were the same as used in the dimer MRCI calculations and also the choice of monomer orbitals that were kept doubly occupied or put into the active space was the same as in the dimer calculations. For OH we computed matrix elements $\langle\Lambda'|Q^{L_A}_{\Lambda'-\Lambda}|\Lambda\rangle$ with $\Lambda', \Lambda=\pm1$ for $L_A=1$, 2,3. For HCl we computed multipole moments $\langle Q_0^{L_B}\rangle$ for $L_B=1,2,3$. The values obtained are listed in Table I. Hence, the long range diabatic potentials that were obtained from the multipole expansion contain terms up to R^{-7}, inclusive, but only the terms up to R^{-5} inclusive are complete. We already observed that the leading term in the diagonal potential $V_{1,1}$ is the dipole-dipole term $\propto R^{-3}$, whereas the off-diagonal potential $V_{1,-1}$ has the quadrupole-dipole term $\propto R^{-4}$ as its leading long range contribution.

Downloaded 01 Jun 2012 to 131.174.17.23. Redistribution subject to AIP license or copyright; see http://jcp.aip.org/about/rights_and_permissions

TABLE I. Multipole matrix elements of OH($^2\Pi$) and multipole moments of HCl. Values in atomic units $e(a_0)^L$, defined with the diatoms oriented along the z-axis, the origin at the center of mass, and the H atoms on the positive side. Literature values for the dipole moment of OH and the dipole, quadrupole, and octupole of HCl are given in parentheses.

L	$\Lambda'-\Lambda$	$\langle\Lambda'\vert Q^L_{\Lambda'-\Lambda}\vert\Lambda\rangle$
OH ($\Lambda',\Lambda=\pm1$)		
1	0	0.6545 [0.6512 (Refs. 26 and 27)]
2	2	−1.1825
2	−2	−1.1825
2	0	1.3939
3	0	2.6691
3	2	0.7986
3	−2	0.7986
HCl ($\Lambda'=\Lambda=0$)		
1	0	0.4443 [0.4344 (Ref. 28, 0.4720 (Ref. 28)]
2	0	2.6972 [2.732 (Ref. 28), 2.756 (Ref. 29)]
3	0	3.9537 [3.886 (Ref. 28)]

IV. FIT OF THE DPES

In this section will be described how the expansion coefficients $v^{\Lambda'\Lambda}_{L_AL_BM}$ and $v^{\Lambda'\Lambda}_{L_AL_BL}$ appearing in Eqs. (28) and (27), respectively, were determined. Most of the programs that perform this task were coded in the commercial program package Matlab.[20] Both expansions of the DPESs require associated Legendre polynomials $C^L_M(\theta,0)\equiv P^L_M(\cos\theta)$ and "Wigner d functions" $d^j_{m'm}(\theta)\equiv D^j_{m'm}(0,\theta,0)$ (also known as "reduced rotation matrix elements"[21]). The functions P^L_M are well-known and easily calculated by recursion; they are also part of Matlab. The d functions may be written as[22]

$$d^j_{m'm}(\theta)=(-1)^\lambda\binom{2j-k}{k+\alpha}^{1/2}\binom{k+\alpha}{\beta}^{-1/2}\left(\sin\frac{\theta}{2}\right)^\alpha\times\left(\cos\frac{\theta}{2}\right)^\beta P^{(\alpha,\beta)}_k(\cos\theta), \tag{47}$$

where $P^{(\alpha,\beta)}_k(\cos\theta)$ is a Jacobi polynomial. Here $k=\min(j+m,j-m,j+m',j-m')$. The phase λ and the index α are given by

$$\text{if } k=\begin{cases} j+m: & \alpha=m'-m;\ \lambda=m'-m\\ j-m: & \alpha=m-m';\ \lambda=0\\ j+m': & \alpha=m-m';\ \lambda=0\\ j-m': & \alpha=m'-m;\ \lambda=m'-m\end{cases}.$$

The index $\beta=2j-2k-\alpha$. Fortran-90 and Matlab routines for a variety of polynomials are available on the internet,[23] among which is a routine for Jacobi polynomials. Use of this routine together with Eq. (47) gives a stable and efficient algorithm for the generation of the d functions.

Since for the smallest values of R the potential becomes extremely repulsive for certain orientations of the OH and HCl monomers, one would need very many terms in the expansion. To avoid this, the potential $V_{1,1}$ was damped in these strongly repulsive regions by means of a tanh function up to a value $V_{\max}$

$$\tilde V_{1,1}=\begin{cases} V_{1,1} & \text{for } V_{1,1}\leqslant V_0\\ V_0+\beta^{-1}\tanh[\beta(V_{1,1}-V_0)] & \text{for } V_{1,1}>V_0\end{cases}, \tag{48}$$

where $\beta\equiv[V_{\max}-V_0]^{-1}$. With this scheme, the damped potential $\tilde V_{1,1}$ is continuous around V_0 up to the second derivative. Care was taken to use sufficiently high values of V_0 and $V_{\max}$, so that the potential was affected only in regions that are not of any practical importance in bound state and scattering calculations. The actual values used were $V_0=10\,000\ \text{cm}^{-1}$, and $V_{\max}=2V_0$. At those grid points where $V_{1,1}$ was damped the off-diagonal potential $V_{1,-1}$ was scaled by the same factor $\tilde V_{1,1}/V_{1,1}$.

We experimented with two different fitting strategies: (i) radial fits of the energies $V_{1,1}$ and $V_{1,-1}$ followed by angular expansions of the radial fit parameters and (ii) angular fits of the energies followed by radial fits of the angular fit parameters. Overall the second strategy gave the more accurate fit and—after the fit parameters are determined—the fastest program for generation of the fitted DPESs. For both the real $V_{1,1}$ and the complex $V_{1,-1}$ the fit was first performed for the coefficients in the *LLM* expansion in Eq. (28).

Since the *LLM* expansion is in terms of orthogonal functions, each expansion (or Fourier) coefficient can be looked upon as an overlap integral between the function to be expanded and one of the expansion functions. This means that the coefficients can be obtained by numerical integration. Before actually performing this integration we generated values of the potentials $V_{1,1}$ and $V_{1,-1}$ on a 10-point Gauss–Legendre (GL) quadrature grid for both θ_A and θ_B by interpolating the 13×13 (θ_A,θ_B) *ab initio* points. A two-dimensional cubic spline interpolation method was used for this purpose. In order to avoid the oscillations that may occur in a cubic spline method especially near the boundaries of the interval to be interpolated we extended the range of θ_A and θ_B from $0\leqslant\theta\leqslant\pi$ to $-\pi\leqslant\theta\leqslant2\pi$. The values of the potentials for $-\pi\leqslant\theta\leqslant0$ and for $\pi\leqslant\theta\leqslant2\pi$ were obtained from the original values for $0\leqslant\theta\leqslant\pi$ by means of the transformations

$$V_{1,\pm1}(R,\theta_A,\theta_B,\phi)=V_{1,\pm1}(R,2\pi-\theta_A,\theta_B,\pi+\phi)=V_{1,\pm1}(R,\theta_A,2\pi-\theta_B,\pi+\phi), \tag{49}$$

which are simply a consequence of the periodic boundary conditions in spherical polar coordinates, and the property that the addition of $\pm2\pi$ to any of these angles makes no difference. In addition, we used that $V_{1,1}(R,\theta_A,\theta_B,\phi)=V_{1,1}(R,\theta_A,\theta_B,-\phi)$ and $V_{1,-1}(R,\theta_A,\theta_B,\phi)=V_{1,-1}(R,\theta_A,\theta_B,-\phi)^*$, which follows from the reflection symmetry treated in Sec. II C. Next the integration was performed by means of a 10-point GL quadrature for θ_A and θ_B (in the range $0\leqslant\theta_A,\theta_B\leqslant\pi$) and a 5-point trapezoidal rule for ϕ. From Eq. (36) follows that in the *LLM* expansion of the diagonal ($\Lambda'=\Lambda$) potential $V_{1,1}$ only non-negative M values appear. Expansion coefficients $v^{1,1}_{L_AL_BM}(R_i)$ with maximum $L_A,L_B=7$ and $M=0$, 1,2,3,4 were computed. In the off-diagonal potential $V_{1,-1}$ also negative M values appear. We computed expansion coefficients $v^{1,-1}_{L_AL_BM}(R_i)$ with maximum $L_A,L_B=7$ and $M=-4,-3,\cdots,4$. All of these coefficients were obtained on

Downloaded 01 Jun 2012 to 131.174.17.23. Redistribution subject to AIP license or copyright; see http://jcp.aip.org/about/rights_and_permissions

the R grid. Note that the expansion coefficients are real-valued, even for the complex-valued potential $V_{1,-1}$; the overlap integrals to be evaluated in that case contain both the real and imaginary parts of $V_{1,-1}$ and the real and imaginary parts of the expansion functions.

Once the coefficients $v^{\Lambda'\Lambda}_{L_A L_B M}(R_i)$ in the *LLM* expansions were obtained, the coefficients $v^{\Lambda'\Lambda}_{L_A L_B L}(R_i)$ in the *LLL* expansions were computed from Eq. (30). As just stated, in the case of the diagonal potential $V_{\Lambda\Lambda}$ the *LLM* coefficients on the right-hand side of this equation are only determined for non-negative M. From the properties of the expansion coefficients derived in Sec. II C it follows that the diagonal coefficients $v^{\Lambda\Lambda}_{L_A L_B L}$ vanish unless L_A+L_B+L is even. For given L_A, L_B the number of L values with even L_A+L_B+L allowed by the triangular relation is equal to the number of non-negative M values. Separating the summation in Eq. (30) in one over positive M and one over negative M, using Eq. (36), we find that for odd L_A+L_B+L the expansion coefficients $v^{\Lambda\Lambda}_{L_A L_B L}$ indeed vanish and that for even L_A+L_B+L:

$$v^{\Lambda\Lambda}_{L_A L_B L} = \sum_{M \geqslant 0} (2-\delta_{M0}) \langle L,0 \mid L_A,M;L_B,-M\rangle v^{\Lambda\Lambda}_{L_A L_B M}.$$

Finally, the angular expansion coefficients $v^{\Lambda'\Lambda}_{L_A L_B L}(R)$ were fitted as functions of R by means of the reproducing kernel Hilbert space (RKHS) method[24] with the reproducing kernel for distance-like variables. The dominant proportional ($\propto R^{-3}$) contribution to the diagonal potential $V_{1,1}$ in the long range is given by the dipole-dipole interaction with $L_A=1$ and $L_B=1$, see Sec. II F. The dominant ($\propto R^{-4}$) long range contribution to the off-diagonal potential $V_{1,-1}$ is the quadrupole-dipole interaction with $L_A=2$ and $L_B=1$. All contributions with $L_A+L_B<5$, which decay slower than the leading induction and dispersion terms $\propto R^{-6}$, were fitted with RKHS parameter $m=L_A+L_B$, so that they decay as $R^{-L_A-L_B-1}$ (Ref. 24) beyond the outermost grid point. All expansion coefficients with $L_A+L_B+1 \geqslant 6$ were fitted with RKHS parameter $m=5$ and decay as R^{-6} for very large R. The smoothness parameter n was always 2. The Fortran code with the fitted diabatic potentials is available from the authors upon request.

V. RESULTS AND DISCUSSION

Before we discuss the potentials obtained we mention some results regarding the accuracy of the analytic potentials with respect to the original *ab initio* data. For a distance R of 3.5 Å the mean absolute error in the diagonal diabatic potential $V_{1,1}$ is 30.8 cm^{-1}, which is about 8% of the average magnitude of $V_{1,1}$ at this distance. The mean absolute error in the off-diagonal potential $V_{1,-1}$ is 11.5 cm^{-1}, while the average of $|V_{1,-1}|$ is 82 cm^{-1} at $R=3.5$ Å. At $R=10$ Å the mean absolute error in $V_{1,1}$ is 0.4 cm^{-1}, which is about 4% of the magnitude of $V_{1,1}$. The mean absolute error in $V_{1,-1}$ at $R=10$ Å is 0.05 cm^{-1}, while the average of $|V_{1,-1}|$ is 0.7 cm^{-1}.

First we discuss the diabatic potentials at $R=3.5$ Å, which is close to the distance of the hydrogen-bonded equilibrium geometry. Figure 2 shows the diagonal potential $V_{1,1}$ for planar geometries with $\phi=0°$ and $\phi=180°$, while Fig. 3 shows the same potential at dihedral angle $\phi=90°$. The minimum of -901 cm^{-1} occurs at $\phi=180°, \theta_{\text{OH}}=150°$, and $\theta_{\text{ClH}}=176°$. When relaxing the distance R we find a binding energy of 905 cm^{-1} at $R=3.45$ Å and nearly the same angles. This corresponds to a nearly linear hydrogen bonded structure with HCl being the proton donor in the hydrogen bond and OH being the proton acceptor. The donor HCl molecule lies nearly along the bond, the acceptor OH radical makes an angle of 150° with the bond axis. This OH angle will change substantially when we include the off-diagonal potential and consider the minimum in the lowest adiabatic potential, see Fig. 1 and the discussion below. A second (meta)stable struc-

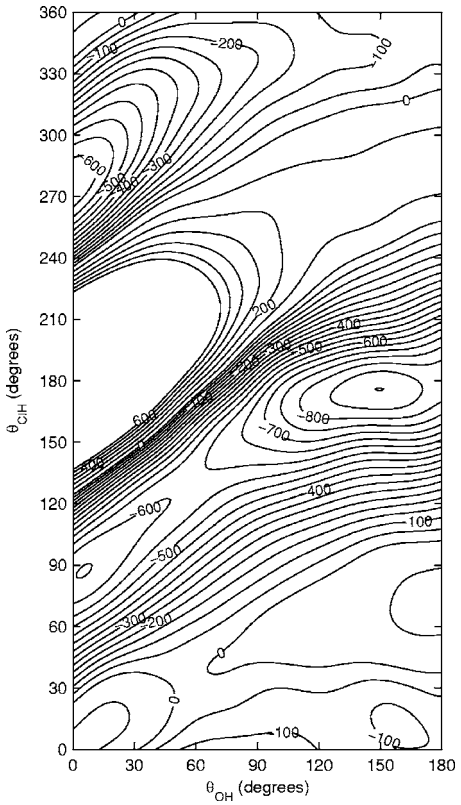

FIG. 2. Diabatic potential $V_{1,1}$ (in cm^{-1}) at $R=3.5$ Å for planar geometries. The lower half of the figure for $0° \leqslant \theta_{\text{ClH}} \leqslant 180°$ corresponds to $\phi=180°$, the upper half for $180° \leqslant \theta_{\text{ClH}} \leqslant 360°$ corresponds to $\phi=0°$ values of $V_{1,1}$ transformed with the aid of Eq. (49).

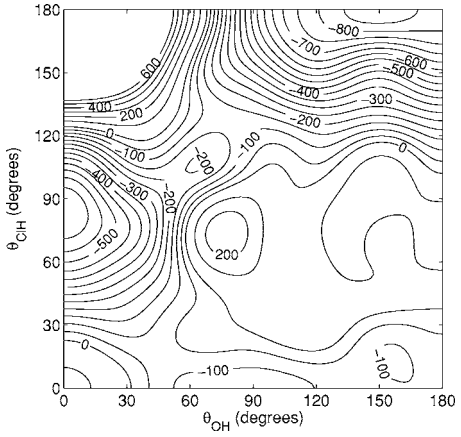

FIG. 3. Diabatic potential $V_{1,1}$ (in cm^{-1}) for $\phi=90°$ and $R=3.5$ Å.

Downloaded 01 Jun 2012 to 131.174.17.23. Redistribution subject to AIP license or copyright; see http://jcp.aip.org/about/rights_and_permissions

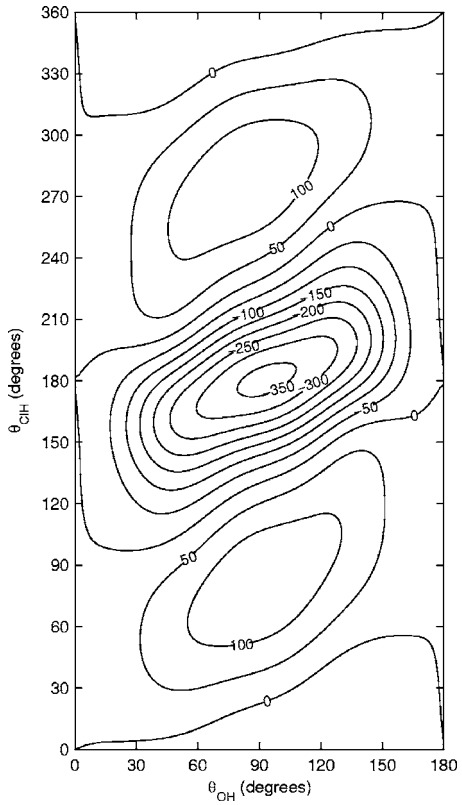

FIG. 4. (Real-valued) diabatic potential $V_{1,-1}$ (in cm^{-1}) at $R=3.5$ Å for planar geometries with $\phi=180°$ and $\phi=0°$, put together as described in Fig. 2.

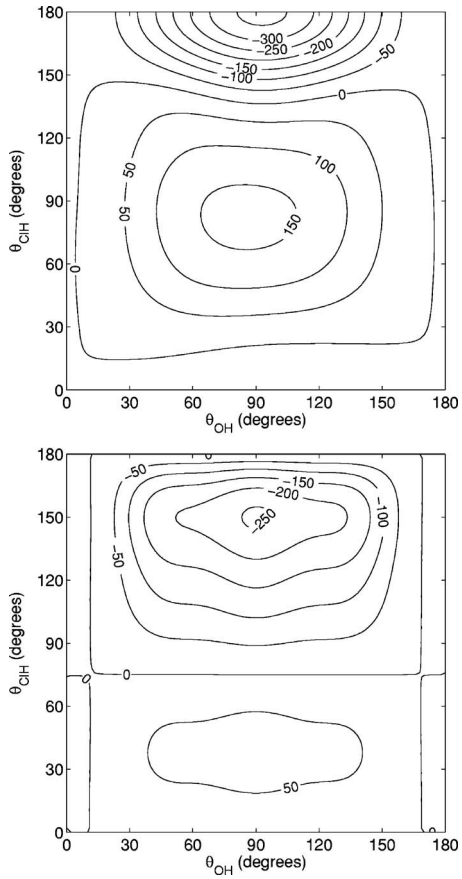

FIG. 5. Real (upper panel) and imaginary (lower panel) part of diabatic potential $V_{1,-1}$ (in cm^{-1}) for $\phi=90°$ and $R=3.5$ Å.

ture occurs for the hydrogen bonded geometry with $\phi=180°$, $\theta_{OH}=4°$ and $\theta_{ClH}=87°$. This geometry corresponds to a hydrogen bond with OH as the donor and HCl as the acceptor. The binding energy of 653 cm^{-1} at the optimized distance $R=3.52$ Å is substantially smaller than for the most stable hydrogen bonded geometry. As in the HCl-HCl dimer,[25] the accepting HCl molecule is nearly perpendicular to the bond axis. This is due to the relatively large quadrupole moment of HCl that prefers to align itself perpendicularly to the dipole of OH.

Figure 4 shows the off-diagonal potential $V_{1,-1}$ at $R=3.5$ Å for planar geometries with $\phi=0°$ and $\phi=180°$, where it is real-valued. Figure 4 shows the real and imaginary parts of this potential at dihedral angle $\phi=90°$. It is clear that the imaginary part is as important as the real part. The largest absolute values occur near $\theta_{OH}=90°$ and $\theta_{ClH}=180°$, i.e., for T-shaped geometries with HCl along the bond axis and its hydrogen atom pointing to the OH center of mass. For planar geometries with $\theta_{ClH}=0°$ or 180° the potential $V_{1,-1}$ must be real-valued for all values of θ_{OH}, because of the A' and A'' reflection symmetry of the real diabatic states $|\Pi_x\rangle$ and $|\Pi_y\rangle$ and the fact that the plane of reflection is the xz-plane. For linear geometries, with both OH and HCl lying along the bond axis, the $|\Pi_x\rangle$ and $|\Pi_x\rangle$ states are degenerate and the off-diagonal potential $V_{1,-1}$ vanishes altogether. For planar geometries with $\theta_{OH}=0°$ and HCl not lying along the bond axis, the diabatic mixing angle γ must equal the dihedral angle ϕ. Analogously, $\gamma=-\phi$ when $\theta_{OH}=180°$. Since the phase of the potential $V_{1,-1}$ is $\exp(2i\gamma)$, see Eq. (4), this potential is real-valued at $\phi=90°$ and purely imaginary at $\phi=45°$ and 135°. This is a consequence of the A' and A'' reflection symmetry of the adiabatic states when the complex is planar. For $\phi=0°$ the adiabatic states coincide with the real diabatic states $|\Pi_x\rangle$ and $|\Pi_y\rangle$, whereas for other values of ϕ the complex is still planar when OH lies along the bond axis, but the plane of reflection has rotated over an angle ϕ with respect to the xz-plane. Hence, also the adiabatic states have rotated over ϕ with respect to the bond axis. The diabatic states $|\Pi_x\rangle$ and $|\Pi_y\rangle$ remain (anti)symmetric with respect to the xz-plane and Eq. (1) tells us that the diabatic mixing angle γ equals ϕ for $\theta_{OH}=0°$ and $-\phi$ for $\theta_{OH}=180°$.

An algebraic proof of these special relations for geometries where one or both of the monomers lie along the bond axis follows directly from the analytic expansion formulas in Sec. II E. When $\theta_{ClH}=0°$ or 180° we use the property of spherical harmonics that $C_M^L(0,\phi)=\delta_{M,0}$ and $C_M^L(\pi,\phi)=(-1)^L\delta_{M,0}$. Hence, the angular expansion functions, and also the potentials $V_{1,1}$ and $V_{1,-1}$, then do not depend on ϕ. When $\theta_{OH}=0°$ or 180° we use the property of Wigner D-functions that $D_{M,K}^L(\phi,0,0)^*=\delta_{M,K}\exp(iK\phi)$ and $D_{M,K}^L(\phi,\pi,0)^*=(-1)^{L-K}\delta_{M,-K}\exp(-ik\phi)$. The diagonal potential $V_{1,1}$ must be expanded in angular functions with $K=0$ and does not depend on ϕ when $\theta_{OH}=0°$ or 180°. The off-diagonal potential $V_{1,-1}$ must be expanded in angular functions with $K=2$ and, hence, contains the complex-valued factor $\exp(2i\phi)$ when $\theta_{OH}=0°$ or $\exp(-2i\phi)$ when θ_{OH}

Downloaded 01 Jun 2012 to 131.174.17.23. Redistribution subject to AIP license or copyright; see http://jcp.aip.org/about/rights_and_permissions

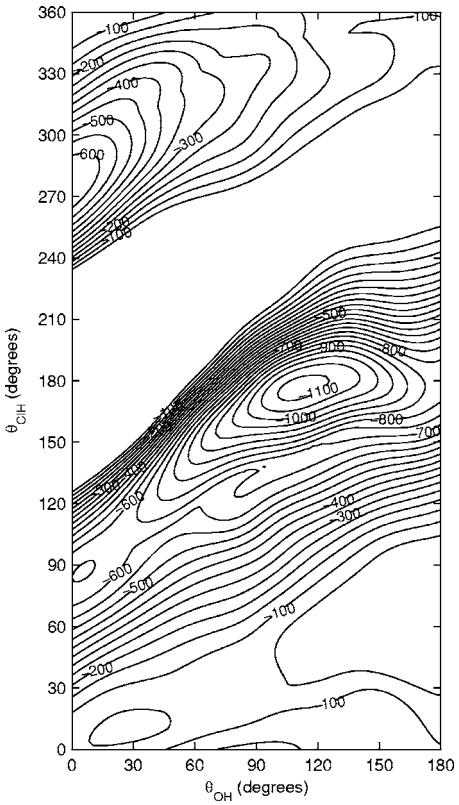

FIG. 6. Lowest adiabatic potential (in cm^{-1}) for optimized R at planar geometries with $\phi=180°$ and $\phi=0°$, put together as described in Fig. 2.

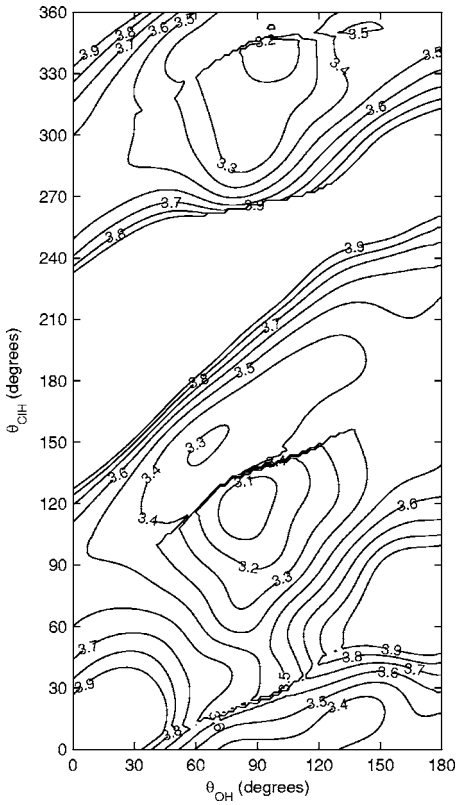

FIG. 7. Equilibrium values of R for the lowest adiabatic potential in Fig. 6 at planar geometries with $\phi=180°$ and $\phi=0°$, put together as described in Fig. 2.

$=180°$. By comparison with Eq. (4) it follows that the diabatic angle γ equals ϕ when $\theta_{OH}=0°$ and $-\phi$ when $\theta_{OH}=180°$.

From Eq. (4) it follows that the lowest adiabatic potential is simply obtained by subtracting the absolute value of $V_{1,-1}$ from $V_{1,1}$. Figure 6 gives a picture of the lowest adiabatic potential for planar geometries with $\phi=0°$ and 180°. This figure shows the minimum value of the lowest adiabatic potential obtained by varying the distance R for each set of angles $\theta_{OH}, \theta_{ClH}, \phi$. The corresponding equilibrium values of R are plotted in Fig. 7. The geometry of the most stable hydrogen bonded structure, see Fig. 1(a), has substantially changed with respect to the minimum in the diagonal potential in Fig. 2. The HCl molecule is still the donor and lies nearly parallel with the bond axis ($\theta_{ClH}=176.4°, \phi=180°$), but the acceptor OH now makes an angle θ_{OH} of 110.7° with the bond axis. The binding energy is $D_e=1123\ cm^{-1}$ and the equilibrium distance is $R_e=3.366$ Å. We still find a second, metastable, hydrogen bonded structures, see Fig. 1(b), with OH as the donor and HCl as the acceptor at $\theta_{OH}=5.5°$, $\theta_{ClH}=86.9°$, $\phi=180°$, $R_e=3.517$ Å, and $D_e=655\ cm^{-1}$.

The earlier calculations of the potential energy surface of $OH+HCl \rightarrow H_2O+Cl$ (Refs. 2–6) concentrate on the transition state for the reaction in which the HCl bond is substantially elongated with respect to free HCl, so we cannot compare the results with those of the present paper. The paper by Yu and Nyman[2] also contains *ab initio* results for the geometry and energetics of the OH–HCl entrance channel complex. These authors performed second-order Møller–Plesset (MP2) calculations on the planar complex in a fairly small basis. They correct for the omission of BSSE corrections and incomplete correlation by a scaling method. Thus, they find a minimum energy of the complex of 5.46 kcal/mol $=1910\ cm^{-1}$ at (in our coordinates) $\theta_{OH}=112.8°$ and $\theta_{ClH}=163.5°$ with a distance between the centers of mass of 4.334 $a_0=2.294$ Å. These equilibrium angles are not very different from ours, but compared to our results their minimum is considerably too deep and falls at too short a distance. The most likely source of this discrepancy is that their scaling method does not correct sufficiently for the BSSE.

In Figs. 8–11 we display the diabatic potentials at $R=10$ Å and compare them with the corresponding potentials directly calculated from the multipole expansion with the multipole moments of Table I and the formulas of Sec. II F. Both the diagonal potential $V_{1,1}$ and the off-diagonal potential $V_{1,-1}$ agree very well with their multipole-expanded counterparts. One observes this for planar geometries with $\phi=0°$ and 180° in Fig. 8 for the diagonal potential $V_{1,1}$ and in Fig. 9 for the off-diagonal potential $V_{1,-1}$. It holds also for non-planar geometries where the off-diagonal potential $V_{1,-1}$ is complex-valued, see Fig. 10 for $V_{1,1}$ and Fig. 11 for the real and imaginary parts of $V_{1,-1}$. At this large distance of 10 Å the dipole-dipole interactions dominate the potential $V_{1,1}$ and the most stable structure corresponds to $\theta_{OH}=180°$ and $\theta_{ClH}=180°$, i.e., to a linear geometry with the HCl and OH dipoles both aligned along the bond axis. The largest absolute (negative) values of $V_{1,-1}$, the leading term of which is the OH quadrupole–HCl dipole interaction, occur for $\theta_{OH}=90°$ and $\theta_{ClH}=180°$.

Downloaded 01 Jun 2012 to 131.174.17.23. Redistribution subject to AIP license or copyright; see http://jcp.aip.org/about/rights_and_permissions

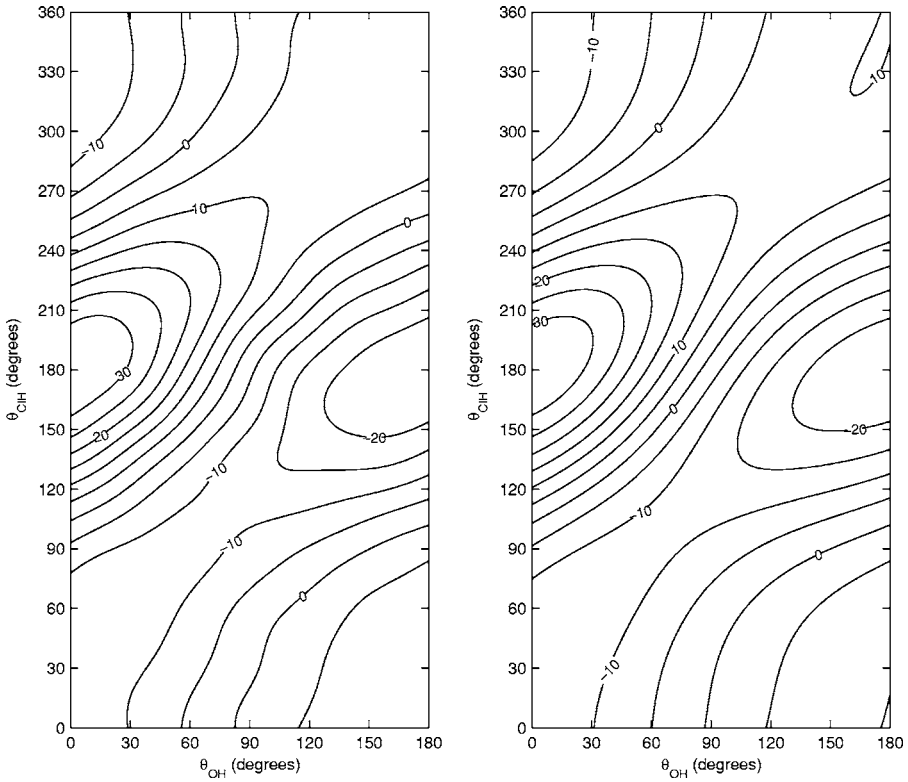

FIG. 8. Diabatic potential $V_{1,1}$ (in cm^{-1}) at $R=10$ Å for planar geometries with $\phi=180°$ and $\phi=0°$, put together as described in Fig. 2. From the full *ab initio* calculations (left panel) and from the multipole expansion (right panel).

In Fig. 12 we show that the multipole-expanded potentials agree with the *ab initio* values for large R. For the OH and HCl angles in these plots we chose the angles of the most stable hydrogen-bonded structure. With decreasing R the attractive dispersion interactions, not included in the first-order multipole expansion, become important and at small R the repulsive exchange interactions dominate.

VI. SUMMARY AND CONCLUSIONS

We have reported *ab initio* computations of the diabatic potential energy surfaces (DPESs) $V_{1,1}(R,\theta_A,\theta_B,\phi)$ and $V_{1,-1}(R,\theta_A,\theta_B,\phi)$ for the dimer $OH(^2\Pi)$–HCl. The DPESs are obtained from the lowest two adiabatic surfaces by combining results from RCCSD(T) and MRCI calculations: The

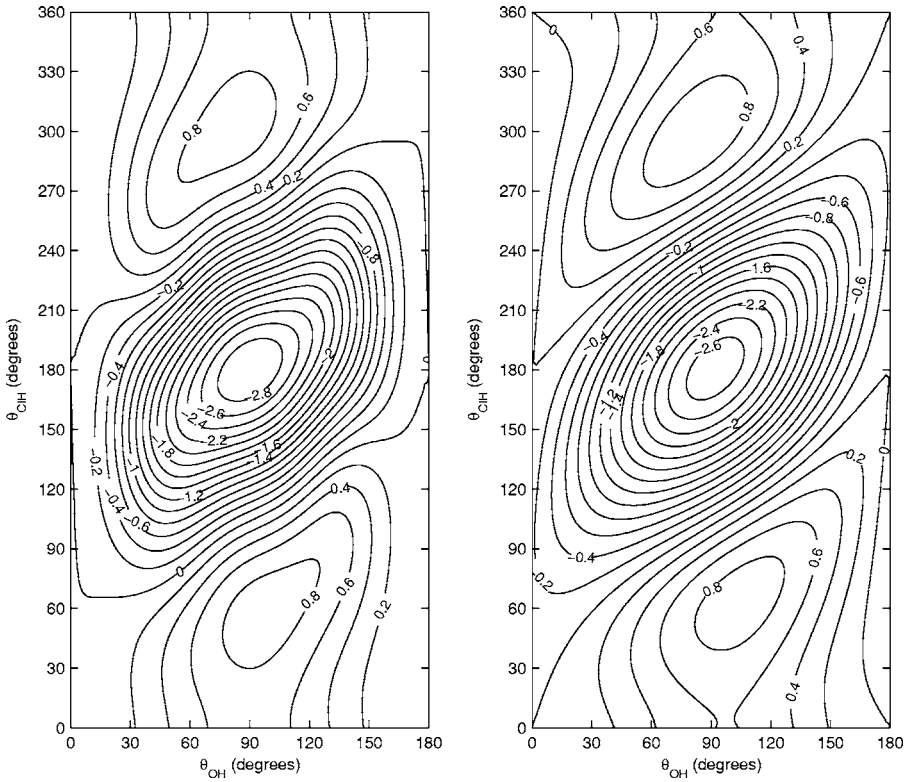

FIG. 9. (Real-valued) diabatic potential $V_{1,-1}$ (in cm^{-1}) at $R=10$ Å for planar geometries with $\phi=180°$ and $\phi=0°$, put together as described in Fig. 2. From the full *ab initio* calculations (left panel) and from the multipole expansion (right panel).

Downloaded 01 Jun 2012 to 131.174.17.23. Redistribution subject to AIP license or copyright; see http://jcp.aip.org/about/rights_and_permissions

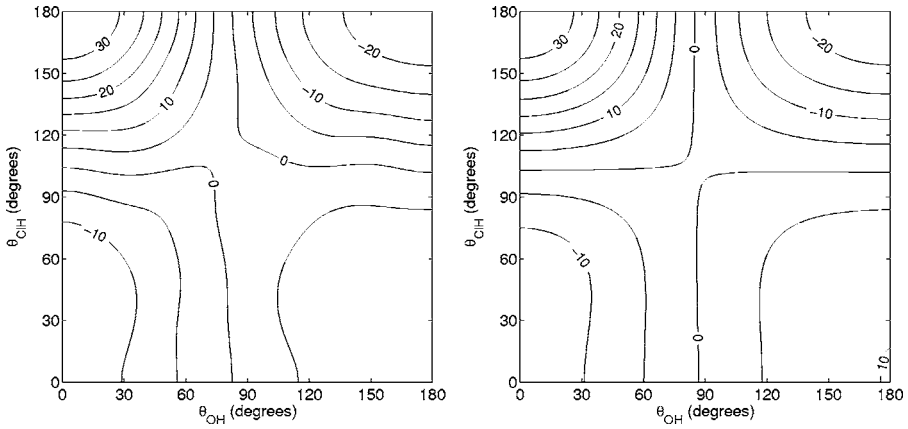

FIG. 10. Diabatic potential $V_{1,1}$ (in cm^{-1}) for $\phi=90°$ and $R=10$ Å. From the full *ab initio* calculations (left panel) and from the multipole expansion (right panel).

RCCSD(T) method gives the ground state energy, while the first excitation energy is computed by the MRCI method. Diabatic states are obtained from the lowest two adiabatic states by a 2×2 rotation with rotation angle γ, the so-called "diabatic angle". The diabatic angle is obtained from inspection of CASSCF natural orbitals and MRCI states.

The two DPESs thus obtained are expanded in terms of orthogonal polynomials depending on the angles θ_A, θ_B, and ϕ. The form of this expansion is suggested by the electrostatic interaction between the monomers, one of which has a spatially degenerate Π ground state. It is shown that the *ab initio* results converge for large R to the electrostatic interactions, so that the expansion of the DPES coincides asymptotically with the multipole expansion of the electrostatic interaction.

Some experimentation with the numerical calculation of the angular expansion coefficients led to a scheme in which the *ab initio* points are first spline-interpolated to Gauss–Legendre quadrature points. In this interpolation it turns out to be useful to continue the colatitude angles θ_A and θ_B on the sphere from $-\pi$ to 2π. The expansion coefficients were then computed by a Gauss–Legendre quadrature, which is possible by virtue of the fact that the expansion is in terms of orthogonal polynomials. Finally, the angular expansion coefficients are given as functions of R by the reproducing kernel Hilbert space method. The diabatic and adiabatic PESs are discussed and some representative cuts are shown.

Bound state and scattering calculations are in progress; comparison of the results of these ongoing computations with experimental data will provide useful information on the OH–HCl entrance channel complex of the chemical reaction $OH+HCl\rightarrow H_2O+Cl$ and, at the same time, decide on the quality of the PESs reported on in this paper.

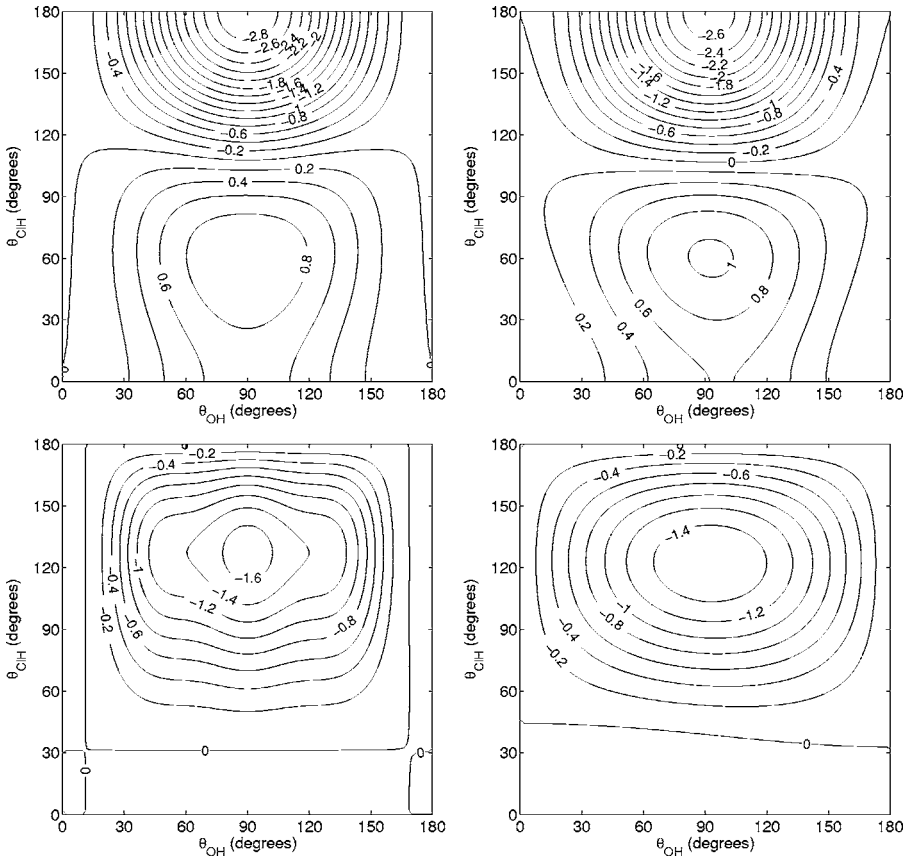

FIG. 11. Real and imaginary parts of diabatic potential $V_{1,-1}$ (in cm^{-1}) for $\phi=90°$ and $R=10$ Å. From the full *ab initio* calculations (left panels) and from the multipole expansion (right panels).

Downloaded 01 Jun 2012 to 131.174.17.23. Redistribution subject to AIP license or copyright; see http://jcp.aip.org/about/rights_and_permissions

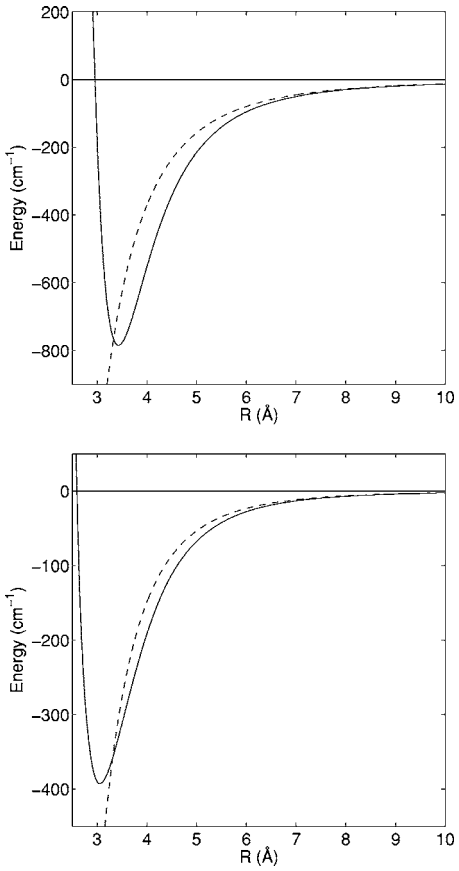

FIG. 12. Potentials $V_{1,1}$ (upper panel) and $V_{1,-1}$ (lower panel) from the full *ab initio* calculations (closed curves) and from the multipole expansion (dashed curves). The angles are the values of the most stable hydrogen-bonded structure: $\theta_{OH}=110.7°$, $\theta_{ClH}=176.4°$, $\phi=180°$.

ACKNOWLEDGMENT

J. Kłos acknowledges financial support from the European Research Training Network THEONET II.

[1] R. Cireasa, M. C. van Beek, A. Moise, and J. J. ter Meulen, J. Chem. Phys. **122**, 074319 (2005).
[2] H.-G. Yu and G. Nyman, J. Chem. Phys. **113**, 8936 (2000).
[3] D. C. Clary, G. Nyman, and E. Hernandez, J. Chem. Phys. **101**, 3704 (1994).
[4] R. Steckler, G. M. Thurman, J. D. Watts, and R. J. Bartlett, J. Chem. Phys. **106**, 3926 (1997).
[5] A. Rodriguez, E. Garcia, M. L. Hernández, and A. Laganà, Chem. Phys. Lett. **360**, 304 (2002).
[6] A. Rodriguez, E. Garcia, M. L. Hernández, and A. Laganà, Chem. Phys. Lett. **371**, 223 (2003).
[7] T. Xie, D. Wang, J. M. Bowman, and D. E. Manolopoulos, J. Chem. Phys. **116**, 7461 (2002).
[8] M. I. Lester (private communication).
[9] F. T. Smith, Phys. Rev. **179**, 111 (1969).
[10] R. Renner, Z. Phys. **92**, 172 (1934), English translation in: H. Hettema, *Quantum Chemistry: Classic Scientific Papers*, (World Scientific, Singapore, 2000).
[11] J. D. Talman, *Special Functions. A Group Theoretic Approach* (W. A. Benjamin, New York, 1968).
[12] A. Messiah, *Quantum Mechanics* (North Holland, Amsterdam, 1969).
[13] S. R. Langhoff and E. R. Davidson, Int. J. Quantum Chem. **8**, 61 (1974).
[14] The aug-cc-pVXZ basis sets were obtained from the Extensible Computational Chemistry Environment Basis Set Database, Version 1.0, as developed and distributed by the Molecular Science Computing Facility, Environmental and Molecular Sciences Laboratory which is part of the Pacific Northwest Laboratory, P.O. Box 999, Richard, Washington 99352, and funded by the U.S. Department of Energy. The Pacific Northwest Laboratory is a multi-program laboratory operated by Battelle Memorial Institute for the U.S. Department of Energy under contract DE-AC06-76RLO 1830.
[15] MOLPRO is a package of *ab initio* programs written by H.-J. Werner and P. J. Knowles, with contributions from J. Almlöf, R. D. Amos, A. Berning *et al.*.
[16] A. Degli Esposti and H.-J. Werner, J. Chem. Phys. **93**, 3351 (1990).
[17] J. Kłos, G. Chałasiński, M. T. Berry, R. A. Kendall, R. Burcl, M. M. Szczęśniak, and S. M. Cybulski, J. Chem. Phys. **112**, 4952 (2000).
[18] G. Herzberg, *Molecular Spectra and Molecular Structure, Vol. 1: Spectra of Diatomic Molecules* (Van Nostrand, New York, 1950).
[19] P.-O. Löwdin, Adv. Quantum Chem. **5**, 185 (1970).
[20] MATLAB Version 6.5, The MathWorks, Inc., 3 Apple Hill Drive, Natick, MA, 2002, http://www.mathworks.com/
[21] M. H. Alexander and G. C. Corey, J. Chem. Phys. **84**, 100 (1986).
[22] L. C. Biedenharn and J. D. Louck, *Angular Momentum in Quantum Physics*, Encyclopedia of Mathematics Vol. 8 (Addison-Wesley, Reading, 1981).
[23] POLPAK - Recursive Polynomials, by J. Burkardt, School for Computational Science, Florida State University.
[24] T.-S. Ho and H. Rabitz, J. Chem. Phys. **104**, 2584 (1996).
[25] M. J. Elrod and R. J. Saykally, J. Chem. Phys. **103**, 933 (1995).
[26] S. R. Langhoff, C. W. Bauschlicher, and P. R. Taylor, J. Chem. Phys. **91**, 5953 (1989).
[27] D. D. Nelson, A. Schiffman, D. J. Nesbitt, J. J. Orlando, and J. B. Burkholder, J. Chem. Phys. **93**, 7003 (1990).
[28] H. Hettema, P. E. S. Wormer, and A. J. Thakkar, Mol. Phys. **80**, 533 (1993).
[29] J. Kłos, G. Chałasiński, M. M. Szczęśniak, and H.-J. Werner, J. Chem. Phys. **115**, 3085 (2001).

Downloaded 01 Jun 2012 to 131.174.17.23. Redistribution subject to AIP license or copyright; see http://jcp.aip.org/about/rights_and_permissions